Skin burns after laser exposure: Histological analysis and predictive simulation

Article *in* Burns: journal of the International Society for Burn Injuries · January 2012

DOI: 10.1016/j.burns.2011.12.006 · Source: PubMed

4 authors, including:

Laetitia Perez
Polytech Angers Angers France
97 PUBLICATIONS **340** CITATIONS
SEE PROFILE

Laurent Autrique
University of Angers
142 PUBLICATIONS **468** CITATIONS
SEE PROFILE

Burns, Volume 38, Issue 5, August 2012, Pages 658–667

Skin burns after laser exposure: histological analysis and predictive simulation

Nathanaëlle MUSEUX [1], Laetitia PEREZ [2], Laurent AUTRIQUE [3], Diane AGAY [4]

[1] DGA/MTO, 10 rue des fours solaires, BP 59, 66121 Font-Romeu, France
e-mail: nathanaelle.museux@dga.defense.gouv.fr

[2] LTN, UMR-CNRS 6607, rue Christian Pauc, BP 50609, 44306 Nantes cedex 3, France
e-mail: laetitia.perez@univ-nantes.fr

[3] Corresponding author, LISA, University of Angers, 62 avenue notre dame du lac, 49000 Angers, France
phone: +33-241-226-518; fax: +33-241-226-561; e-mail: laurent.autrique@univ-angers.fr

[4] IRBA antenne de La Tronche, 24 avenue du Maquis de Grésivaudan, 38702 La Tronche, France
e-mail: diane.agay@crssa.net

Burns, Volume 38, Issue 5, August 2012, Pages 658–667

Abstract

Thermal effects of laser irradiations on skin are investigated in this paper. The main purpose is to determine the damage level induced by a laser exposure. Potential burns induced by two lasers (wavelength 808 nm and 1940 nm) are studied and animal experimentations are performed. Several exposure durations and laser powers are tested. Based on previous works, a mathematical model dedicated to temperature prediction is proposed and finite-element method is implemented. This numerical predictive tool based on the bioheat equation takes into account heat losses due to the convection on skin surface, blood circulatory and also evaporation. Thermal behaviour of each skin layer is also described considering distinct thermal and optical properties. Since mathematical model is able to estimate damage levels, histological analyses are also carried through. It is confirmed that the mathematical model is an efficient predictive tool for estimation of damages caused by burns and that thermal effects sharply depend on laser wavelength.

Keywords

Burn prediction, laser irradiation, thermal analysis

Burns, Volume 38, Issue 5, August 2012, Pages 658–667

1. Introduction

Experimental equipments including laser devices are more and more frequently encountered in medicine (dermatology, surgery, etc.). Besides medical utilities, lasers also take place in guidance systems, measurement devices, weapons, etc. In such a framework, a crucial requirement lies in the estimation of the potential damages due to an accidental exposure. Laser beam thermal effect strongly depends on chromophores which act as the skin layers constitutive elements that absorb light at a specific frequency. Then induced damages as well as application domains strongly depend on laser wavelength. Let us mention, for example, emerging applications for 2 µm fiber lasers in medicine and surgery [1]. For such a wavelength, laser radiation does not penetrate deeply into the skin [2], [3] and it is usually considered eye-safe since it is primarily absorbed in the cornea and aqueous humor with insignificant energy reaching the retina [4]. Medical applications are ophthalmology (presbyopia, hyperopia), otolaryngology, orthopedic procedures, etc. Contrariwise to previous surfacic effects, one can consider a second laser (808 nm) for which the most important chromophore is the melanin (a molecule capable for absorbing both ultraviolet and visible wavelengths); see [5] for example. Since melanin is located in the deep layers of the skin, laser effect is not limited to skin superficial layer and numerous applications are developed in dermatology.

In this study, experimental campaigns were conducted considering potential burns induced by both of the lasers mentioned above (wavelength 1940 nm and 808 nm). In [6], thermal effect of 1064 nm and 1552 nm laser has been investigated in vitro for short pulses. Considering great similarities between human and porcine skin, laser effects have been investigated on pigs. In fact, in 1967, Forges pointed out that vascular organization of porcine skin and human are similar [7]. More recently, Sullivan et al. have performed comparisons focused on wound healing between humans, pigs, small mammals and in vitro samples [8]. In the studied situation, it is shown that the concordance between humans and pigs is 78%, while the concordance between humans and small mammals (or in vitro samples) is lower than 60%. Moreover, besides this attractive similarity, the large size of pigs allows the observation of several injuries in the same subject that reduces the experimental variability.

In order to study burn phenomena and to optimize protection with clothes or gels against laser exposure, the development of a numerical predictive tool for the estimation of damages caused by burns is suitable. Such an approach has been considered by Chen et al. [3], [9] who have shown the interest of mathematical model predictions in burn degree estimation. During the last decades, numerous studies have been dedicated to thermal effect modeling in human skin according to burn type and the accuracies of heat exchanges description (several references in relation with such topic are given in the following). For example, in recent works [10] and [11], numerical models are used to predict scald burns. In this communication, the proposed mathematical model is developed in order to describe thermal effects due to laser exposure. Several additional phenomena are taken into account: convection, evaporation on skin surface and heat losses due to the blood circulation.

The paper is organized as follows. Firstly, in vivo experimentations are presented with experimental setup, skin temperature measurements and histological analyses, performed in order to evaluate injuries in comparison with temperature evolution. Then, the propagation of the laser beam in the skin layers is modeled and finite element method is performed to provide numerical simulation. Experimental biological effects are then compared to predicted effects stated by mathematical models, and finally their adequacy is addressed in the conclusion.

2. Animal experimentations

The damages caused by laser exposure were investigated in vivo. In pigs exposed to two lasers (1940 nm and 808 nm), skin temperature evolutions were measured and biopsies were performed to qualify the deepness of the burn injuries.

2.1 Animal experimentations

Two lasers were considered for experimentations. The first one was an infrared laser (1940 nm - IPG photonics, Model TLR-3, maximum power 4W) while the second one was a visible-wavelength laser (808 nm - Optotools, type OTF 60-30 system, maximum power 60W). In Chen et al. [3], gaussian shaped spot sizes are approximately 5, 10 and 15 mm. In order to overcome this limitation, an optical device has been developed to transform the laser beam of Gaussian type in a uniform square shape [12]. It consists in a kaleidoscope (polish aluminum) located after the laser. For the infrared laser (1940 nm), dimensions are 180 mm length with a square cavity of 15 by 15 mm while for the visible-wavelength laser (808 nm) dimensions are 80 mm length with a square cavity of 4 by 4 mm. A flux meter (Gentec-e, Solo PE 12V 800mA; detector: Cooler Master UP19K-110F-H5-DO, 12V 160mA) conduced to laser power measurement at the end of kaleidoscope.

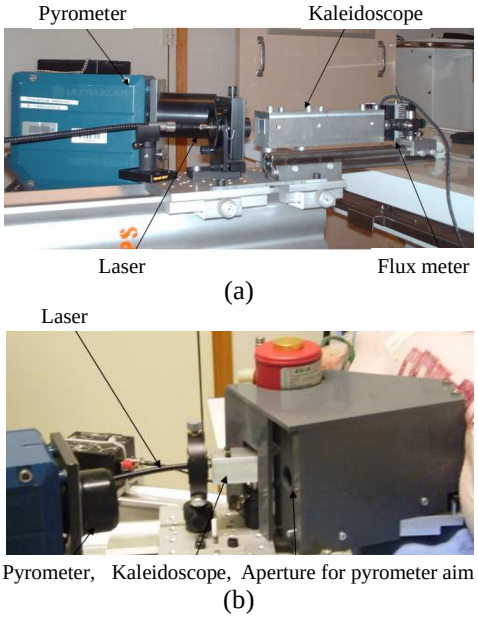

Fig. 1 - Experimental set up for laser exposure (a) 1940 nm laser and (b) 808 nm laser.

Both lasers were driven by a function generator (FG 120 Yokogawa, 2MHz). Surface temperature of the pig skin was measured by an infrared pyrometer (Ultrakust Thermophil INFRAplus®, type R2510-10, focal distance 360 mm in range 8-12 µm, temperature scale 0-200°C). Temperature evolutions were visualized (oscilloscope Tektronix DPO 4104). Experimental setup is shown Fig. 1. Laser spot images have been analyzed (EasyGrab, Scion Image and Origin 6.1 software) in order to verify the spatial uniformity of the incident laser (an example is shown Fig. 2).

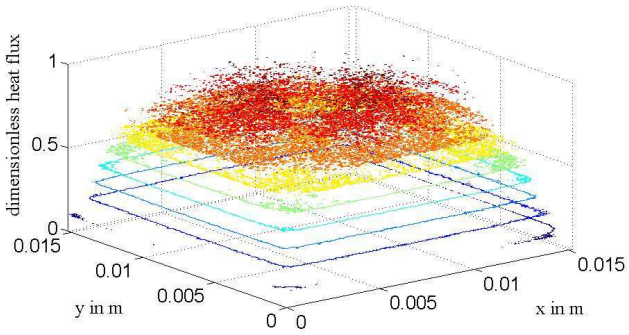

Fig. 2 - Example of laser spatial distribution (kaleidoscope end; laser 1940 nm)

In order to investigate potential damages induced by both of the lasers, several irradiances and exposure durations have been considered (Table 1). These experimental specificities have been chosen according to preparatory tests.

Table 1 - Type of laser exposure (irradiance and duration)

Laser	Duration [s]	Irradiance [kW.m^{-2}]				
1940 nm	$1 \le t_e \le 40$	9.3	10.7	12.2	14.0	
808 nm	$2 \le t_e \le 20$	9.3	14.0	96.4	110.0	122.0

2.2 Protocol

The experimental protocol was approved by the consultative committee for ethics in animal experimentation of the French Army Biomedical Research Institute under the number 2008/14.0. In vivo experiments were performed on six female non pigmented butcher pigs weighing about 23 kg. Each pig was experimented within three days as follows: laser exposures on day 1, clinical observation on day 2, and animal euthanasia and biopsies on day 3. In order to investigate the experimental reproducibility, experimentations were reproduced three times. Thus, twenty five burns of 2.25 cm^2 have been performed on flanks of each animal. On day 1, after sedation by azaperone treatment (50 $mg.kg^{-1}$, Stresnil™, Janssen-Cilag) the animals were anaesthetized by intramuscular injection of a combination of tiletamine and zolazepam (6 $mg.kg^{-1}$, Zoletil 100™, Virbac), and then kept under volatile anaesthesia with a gas mixture of approximately 2% isoflurane (Isuflurane Belamont™, Mundipharma) in oxygen (1 $dm^3.min^{-1}$). Each anaesthetized animal was burned on several locations according to Table I experimental specificities, after that its skin had been shorn and cleaned. During the exposure, skin temperature was measured by a pyrometer. For infrared laser (1940 nm), temperature measurements could be obtained only few seconds after the end of laser irradiation since kaleidoscope edge had been in contact with the skin during the exposure. For the second laser (808 nm), temperature measurements were performed all along the laser exposure and during the skin temperature decreasing. Moreover, in order to observe the blood circulation effect on the skin lesions and the damage levels, seven burns were performed after animals' euthanasia to allow further comparison with perfused tissues. To avoid animal pain, analgesia was performed prior to laser exposure (10 $mg.1ml^{-1}$ of morphine) and extended all along the three days experiment with a transcutaneous patch of fentanyl (50 $\mu g.h^{-1}$, Durogesic™5mg.10cm^{-2}, Janssen-Cilag). The medical observation of the resting animals on day 2 revealed no clinical suffering. On day 3, animal euthanasia was performed by intravenous injection of 20 cm^3 of sodium pentobarbital (Dolethal™, Vétoquinol), and burns biopsies were harvested. The biopsies were fixed in neutral buffered 10% formalin solution (NBF) and stored at +2°C/+8°C. After fixation, the samples were dehydrated in alcohol solutions of increasing concentration, cleared in xylene and embedded in paraffin. Embedded biopsies were cut using a microtome (MICRON®, France). One section (5 µm thickness) per specimen was performed and stained with Hematoxilin Eosin Safran (HES). Qualitative and semi-quantitative histological evaluations of each biopsy were performed and the following parameters were graduated from 0 (absence) to 3 (severe): neutrophilic exocytosis, epidermal necrosis, dermal necrosis, basal lamina necrosis, dermal oedema, dermal congestion/hemorrhage. Moreover, burn severity is defined (Table 2) according to the French Society for Burn Study and Treatment (SFETB) classification (www.sfetb.org).

Table 2 - SFETB classification

Histological grade	Description
1	Superficial epidermis involvement
2	Whole thickness epidermal involvement Basal membrane disruption Papillary dermis involvement
2+	Full-thickness epidermal necrosis, except for hair follicles Partial to complete basal membrane necrosis Reticular dermis involvement
3	Full-thickness epidermal necrosis, including hair follicles Complete basal membrane necrosis Deep dermis/hypodermis involvement

2.3 Experimental results: 1940 nm laser

In fig. 3, temperature evolution of pig skin after the laser exposure is presented for several duration and for the higher irradiance 14 $kW.m^{-2}$. Initial temperature measured on the skin of two pigs is 32.6 ± 0.6°C. Moreover an experimentation has been performed for a 30s burn on a euthanized pig. It is obvious that thermal effect strongly depends on the exposure duration. For example, for a 10s exposure surface temperature decreases below 40°C 38s after the exposure, while for a 20s exposure surface temperature decreases below 40°C 58s after the exposure.

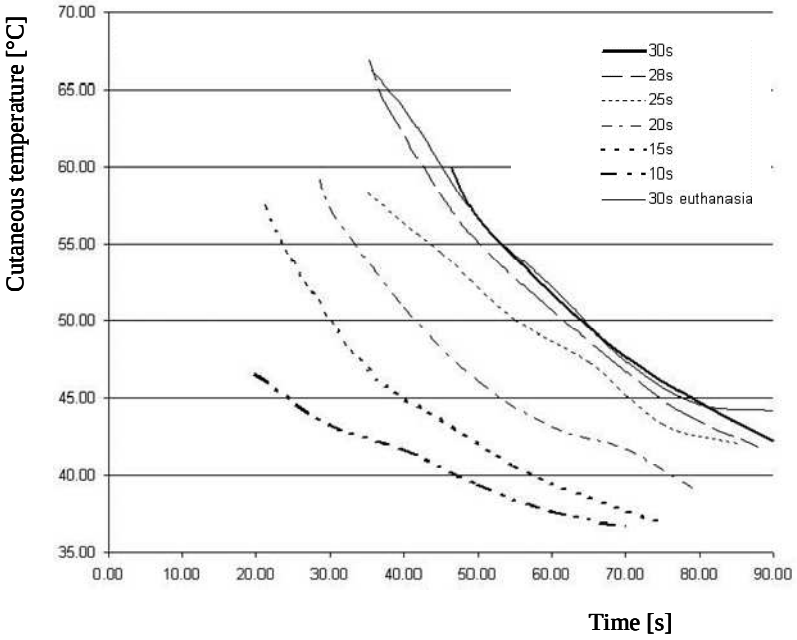

Fig. 3 - Temperature evolution on skin surface: 1940 nm laser exposure, irradiance: 14 $kW.m^{-2}$ **.**

In the exposed configuration (1940 nm laser, 30s exposure, 14 $kW.m^{-2}$), temperature evolutions between euthanized pig and living animal are quite similar. In fact, estimated burn severity corresponds to a severe injury and skin vascularization is no more effective. Moreover for such severe injuries, skin surface inflammation has no heating effect. Biopsies of the damaged tissues are presented in Table 3 for several exposure durations and irradiances. In most cases, third degree burns are observed (full-thickness epidermal necrosis including hair follicles).

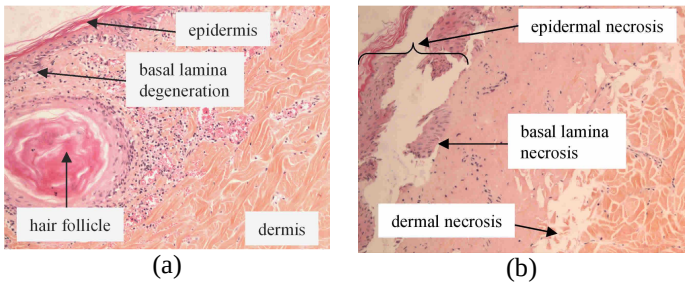

Fig. 4 - Histological pictures, 1940 nm laser exposure, irradiance: 14 $kW.m^{-2}$ **.**
(a) 10s duration (histological grade 2+) (b) 20s duration (histological grade 3)

Table 3 – Burn injury severity (1940 nm Laser)

Irradiance $\left[\text{kW.m}^{-2} \right]$	Exposure duration [s]	Histological grade
9.3	5	0
9.3	15	2+
9.3	20	2+
9.3	25	3
10.7	30	3
12.2	5	0
12.2	10	2+
12.2	15	2+
12.2	20	3
14.0	1	0
14.0	5	0
14.0	10	2+
14.0	15	3
14.0	20	3
14.0	25	3
14.0	28	3
14.0	30	3
euthanized pig 14.0	30	3

The lesion was peracute and consisted of epidermal coagulative necrosis, characterized at the cellular scale by hypereosinophilia, cellular elongation and early nuclear changes (pyknosis mainly). In several instances, dermo-epidermal clefts were observed. The basal membrane was often hypereosinophilic and thickened. Dermal vessels were mildly congested and vascular necrosis as well as nerve fiber necrosis was often observed. For the 2+ gradation, hair follicles were partly damaged and dermal necrosis is more superficial than for third-degree burns (see Fig. 4).

2.4 Experimental results: 808 nm laser

Skin initial temperature of two tested pigs has been measured: 35.1 ± 0.9°C. In this configuration (Fig. 1) skin temperature is also measured during the laser irradiation. Results are shown in Fig. 5 for the higher irradiance $\left(122 \text{ kW.m}^{-2}\right)$.

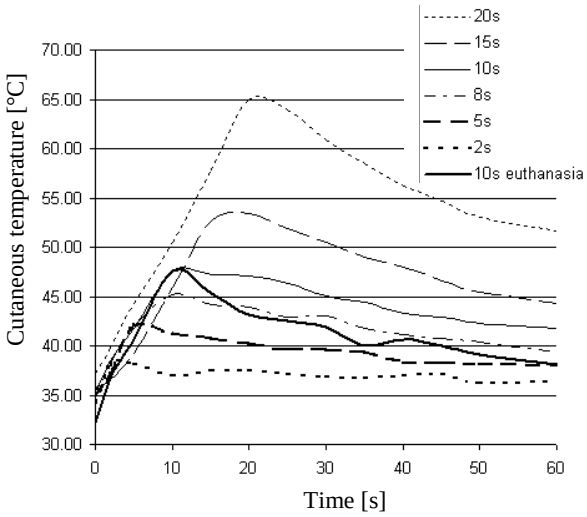

Fig. 5. Temperature evolution on skin surface: 808 nm laser exposure, irradiance: 122 kW.m^{-2} **.**

Moreover, tests have been performed considering alive or euthanized animal with two irradiances 122 kW.m^{-2} and 96 kW.m^{-2} for 10s. Even if the initial temperatures of the euthanized pigs are lower, the skin temperatures

do not increase so much as in lived animals. For such not severe injuries, it seems that skin surface inflammation of living tissues has a heating effect which can not be neglected. For euthanized animal, inflammation does not occur and there is no supplementary heating effect. Moreover, blood perfusion in lived animal limits body temperature increase. Such phenomenon has been taken into account in pioneer works; see for example Pennes heat transfer equation in biological tissues [13].

For weak irradiance $\left(\leq 14\ \mathrm{kW.m^{-2}}\right)$, skin temperature is not dramatically affected whatever the exposure duration is (for such a wavelength). Injury severity is estimated after biopsies (Table 4).

Table 4 – Burn injury severity (808 nm Laser)

Irradiance $\left[\mathrm{kW.m^{-2}}\right]$	Exposure duration [s]	Histological grade
9.3	20	0
14.0	20	0
96.4	5	1
96.4	10	1
110.0	5	1
110.0	10	1
122.0	5	0
122.0	8	0
122.0	10	2
122.0	15	2+
122.0	20	3
euthanized pig 96.4	10	0
euthanized pig 122.0	10	0

For short exposure duration or weak irradiance, a slight focal/multifocal dermal edema is observed in the papillary dermis (under the basal membrane). These observations are not significant enough to state on a first degree burn defined when superficial epidermis is affected with evidences of epidermal pallor or single cell necrosis. Two sites were graded 2 and characterized by focal epidermal degeneration/necrosis, and/or basal lamina disruption leading to dermal-epidermal clefts, and/or an upper dermal edema (slight to moderate). For 2+ gradations, hair follicles are partly affected by the necrotic phenomenon that concerned the surface epithelium or the sweat glands. For three degree burns, in addition to effects mentioned in the previous section, sweat glands also showed coagulation necrosis and cell swelling, as well as epithelial cell sloughing in the glandular lumen. In the upper of the dermis, several sites clearly presented a protein-rich fluid (edema/exudation) between the collagen fibers, while most sites only showed dermal necrosis, characterized by hypereosinophilia of the collagen fibers. Dermal vessels were mildly congested and hemorrhages could be occasionally observed.

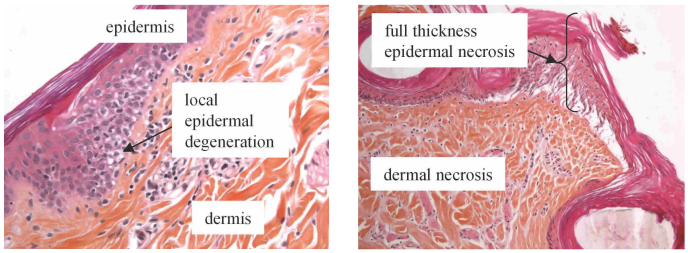

(a) (b)

Fig. 4 - Histological pictures, 808 nm laser exposure, irradiance: 122 $\mathrm{kW.m^{-2}}$ **.**
(a) 10s duration (histological grade 2) (b) 20s duration (histological grade 3)

2.5 Damage comparison caused by both the lasers (1940 and 808 nm)

In order to investigate injuries caused by lasers, several experimentations (same irradiance and same exposure) have been compared and temperature evolution are presented Fig. 7. It is shown that skin temperatures measured just after exposure for the 1940 nm laser are higher than those obtained with the laser of 808 nm.

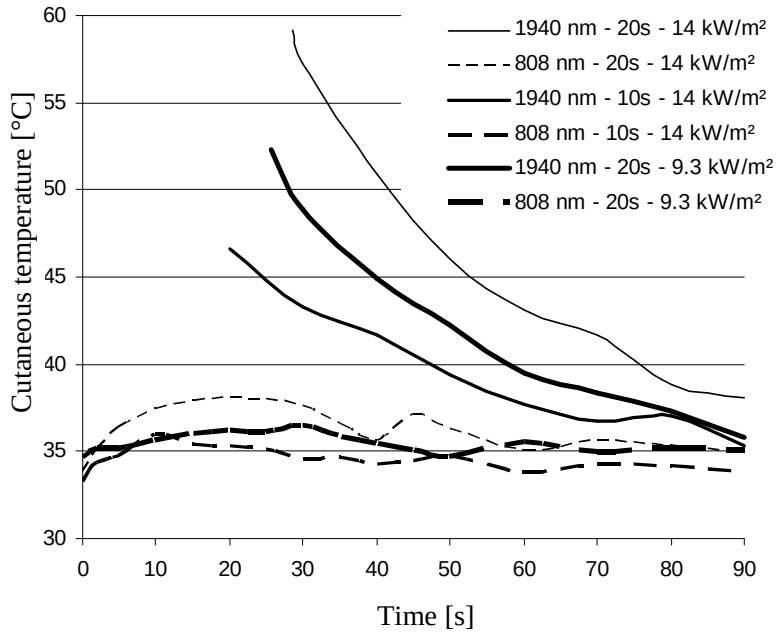

Fig. 7 - Temperature evolution on skin surface: comparison between 1940 nm and 808 nm lasers.

In table 5, temperature differences versus time are given for each experimental condition. Considering table 3, 1940 nm laser leads to 2+ graded injuries for a 20s exposure with 9.3 $kW.m^{-2}$ irradiance or for 10s exposure with 14 $kW.m^{-2}$ irradiance. Moreover, a severe burn (grade 3) is observed for a 20s exposure with 9.3 $kW.m^{-2}$ irradiance with this laser. For the 808 nm laser, no lesions are obtained for these irradiances and exposure durations.

Temperature difference is obviously attenuated during the cooling phase. Similar behaviors have been observed for different experimental conditions.

Such a difference in heating for the two different wavelengths has to be discussed. Skin is deeply affected by 808 nm laser since main chromophore (for this wavelength) is melanin. Melanocytes are located in deep layers thus heat transfer occurs in a larger volume than for the 1940 nm laser. Indeed, for this wavelength, main chromophore is water (constituent of all skin layers) and most of the laser energy is provided at skin surface. Then more important temperature increase is observed on skin surface with 1940 nm laser occurrence (temperature measurements are performed by pyrometer on skin surface).

In the following paragraph, a thermal-damage model is presented in order to develop a predictive tool based on numerical simulation of thermal effect induced by laser exposure.

Table 5 – Comparison of skin temperature versus time for both of the laser (* not measured)

irradiance 9.3 kW.m^{-2} ; exposure duration 20s time after exposure beginning [s]											
	0	10	20	30	40	50	60	70	80	90	
808 nm	34.7	35.6	36.2	36.4	35.4	34.6	35.6	34.9	35.1	35.0	temperature [°C]
1940 nm	32.9	*	*	48.9	44.9	42.2	39.5	38.3	37.3	35.8	temperature [°C]
	-1.8			12.5	9.5	7.6	3.9	3.4	2.2	0.8	difference [°C]
irradiance 14 kW.m^{-2} ; exposure duration 10s time after exposure beginning [s]											
	0	10	20	30	40	50	60	70	80	90	
808 nm	33.2	35.9	35.4	34.6	34.2	34.8	33.8	34.3	34.2	33.7	temperature [°C]
1940 nm	32.9	*	46.6	43.3	41.7	39.4	37.7	36.7	37.0	35.3	temperature [°C]
	-0.3		11.2	8.7	7.5	4.6	3.9	2.4	2.8	1.6	difference [°C]
irradiance 14 kW.m^{-2} ; exposure duration 20s time after exposure beginning [s]											
	0	10	20	30	40	50	60	70	80	90	
808 nm	33.7	37.4	38.1	37.6	35.6	36.2	35.0	35.6	35.4	35.0	temperature [°C]
1940 nm	33.0	*	*	57.3	50.9	46.1	43.1	41.7	38.9	38.1	temperature [°C]
	-0.7			19.7	15.3	9.9	8.1	6.1	3.5	3.1	difference [°C]

3. Thermal-damage mathematical models

Since early works [13] developed by Pennes in 1948, numerous authors have investigated heat transfer in living tissues. Moreover, considering various occurrences (hot gases, conduction, laser, etc.), damage threshold are quite different and safe-exposure limit predictions have to be cautiously considered.

3.1 Heat transfers

The skin is as a multilayer semi-transparent material (epidermis, dermis and hypodermis). The mathematical model presented here after is based on the Pennes heat transfer equation in biological tissues [13]. A 1-dimensional configuration is justified considering the kaleidoscope dimensions ensuring a uniform heating flux on a skin surface greater than biological tissue thickness. Considering conduction, blood circulation and heat generation due to metabolism, the following equation is usually considered:

$$\rho_i c_i \frac{\partial T(x,t)}{\partial t} = k_i \Delta T(x,t) + \omega_i \rho_b c_b \left[T_b - T(x,t)\right] + q_m \qquad (1)$$

where:

- $T(x,t)$ is the temperature in $[\mathrm{K}]$ at depth x in $[\mathrm{m}]$ and time t in $[\mathrm{s}]$,
- $i \in \{e,d,h\}$ corresponds to a specific layer : epidermis $\{e\}$, dermis $\{d\}$ or hypodermis $\{h\}$,
- ρ_i is the density in $\left[\mathrm{kg.m^{-3}}\right]$ of layer i, ρ_b is the blood density in $\left[\mathrm{kg.m^{-3}}\right]$,
- c_i is the specific heat in $\left[\mathrm{J.kg^{-1}.K^{-1}}\right]$,
- k_i is the thermal conductivity in $\left[\mathrm{W.m^{-1}.K^{-1}}\right]$,
- T_b is the blood temperature in $[\mathrm{K}]$ considered as constant,
- q_m is the heat generation in $\left[\mathrm{W.m^{-3}}\right]$ due to the metabolism,
- ω_i is the blood perfusion rate in dermis and hypodermis (in $\left[\mathrm{s^{-1}}\right]$) and is equal to zero in the epidermis.

Blood circulation during burn process is addressed in a later paragraph.

When light scattering can not be neglected, let us consider: $S(x,t) = \beta_{i,\lambda} I(t) \exp(-\beta_{i,\lambda} x)$ where:

- $S(x,t)$ is the localized heat source in $\left[\text{W.m}^{-3}\right]$,
- $\beta_{i,\lambda}$ in $\left[\text{m}^{-1}\right]$ is the scattering coefficient of the layer i (for a given laser wavelength λ),
- $I(t)$ is the laser irradiance $\left[\text{W.m}^{-2}\right]$.

Then, Eq. (1) becomes:

$$\rho_i c_i \frac{\partial T(x,t)}{\partial t} = k_i \Delta T(x,t) + \omega_i \rho_b c_b \left[T_b - T(x,t)\right] + q_m + S(x,t) \qquad (2)$$

Heat exchanges on the skin surface $(x=0)$ take into account natural convection as well as evaporative cooling [3], [14]-[16] and heat losses due to water vaporization are defined as follows:

$$Q_{vap}(t) = \text{H}\, h_m \left(\rho_{v,sat}\left(T(0,t)\right) - \rho_{v,a}\right) \qquad (3)$$

where:

- Q_{vap} is in $\left[\text{W.m}^{-2}\right]$,
- H is the phase change enthalpy $\left[\text{J.kg}^{-1}\right]$,
- h_m is the convection mass transfer coefficient $\left[\text{m.s}^{-1}\right]$. Let us consider [14], [15], $h_m = \frac{h_e}{\rho_a c_a Le^{2/3}}$ where h_e is the heat-convection coefficient $\left[\text{W.m}^{-2}\text{.K}^{-1}\right]$; ρ_a is the air mass density $\left[\text{kg.m}^{-3}\right]$; c_a is the air specific heat $\left[\text{J.kg}^{-1}\text{.K}^{-1}\right]$; Le is the dimensionless Lewis number for the diffusion of water vapor into air. The Lewis number is defined as the ratio between the Schmidt number (*Sc*; dimensionless) and the Prandtl number (*Pr*; dimensionless): $Le = \frac{Sc}{Pr} = \frac{k_a}{D_v \rho_a c_{pa}}$; k_a is the air thermal conductivity in $\left[\text{W.m}^{-1}\text{.K}^{-1}\right]$; D_v is the diffusion coefficient of the water vapor into air $\left[\text{m}^2\text{.s}^{-1}\right]$; c_{pa} is the specific heat of the dry air at constant pressure $\left[\text{J.kg}^{-1}\text{.K}^{-1}\right]$.
- $\rho_{v,sat}$ is the mass density of saturated water vapor $\left[\text{kg.m}^{-3}\right]$ at the temperature of the skin surface $T_s = T(0,t)$. According to Incropera and Dewitt [15], a fourth-order polynomial expression can be considered:

$$\rho_{v,sat}(t) = 4\ 10^{-9} T_s^4 - 6\ 10^{-8} T_s^3 + 1.96\ 10^{-5} T_s^2 + 1.534\,10^{-4} T_s + 6.1098\,10^{-3}$$

- $\rho_{v,a}$ is the density of the water vapor in the air $\left[\text{kg.m}^{-3}\right]$ at the ambient temperature T_a.

Then, in order to model heat exchanges on the skin surface $(x=0)$, the boundary condition is :

$$-k_e \left.\frac{\partial T}{\partial x}\right|_{x=0} = h_e \left(T_a - T(0,t)\right) - Q_{vap}(t) \qquad (4)$$

For free convection in air, h_e usually ranges between 5 and 25 $\text{W.m}^{-2}\text{.K}^{-1}$. Inside the porcine body, a constant temperature (Dirichlet condition) is considered and assumed to be equal to the blood temperature T_b in $\left[\text{K}\right]$. Numerical values taken into account in the mathematical model are given in table 6.

Table 6 – Thermal and optical properties used in the mathematical model

Properties	Localisation	Value	Reference
Thickness $\left[\times 10^{-3}\text{m}\right]$	Epidermis	0.1	Experimental measurement
	Dermis	1.4	
	Hypodermis	> 3.0	
Thermal conductivity k $\left[\text{W.m}^{-1}\text{.K}^{-1}\right]$	Epidermis	0.21	Stolwijk and Hardy [17]
	Dermis	0.42	
	Hypodermis	0.20	Knudsen and Overguard [18] , Cohen [19]
Density ρ $\left[\text{kg.m}^{-3}\right]$	Epidermis	1200	Stolwijk and Hardy [17]
	Dermis	1200	
	Hypodermis	920	
	Blood	1080	Diller and Hayes [20]
Specific heat c $\left[\text{J.kg}^{-1}\text{.K}^{-1}\right]$	Epidermis	3600	Stolwijk and Hardy [17]
	Dermis	3222	Sipe [21]
	Hypodermis	2300	Stolwijk and Hardy [17]
	Blood	3300	Diller and Hayes [20]
Absorption and scattering coefficient β $\left[\text{m}^{-1}\right]$ at 1940nm	Epidermis	2176	Chen et al. [3]
	Dermis	5802	
	Hypodermis	2176	
Absorption and scattering coefficient β $\left[\text{m}^{-1}\right]$ at 808nm	Epidermis	70	Lormel [22]
	Dermis	70	
	Hypodermis	70	
Heat convection h_e $\left[\text{W.m}^{-2}\text{.K}^{-1}\right]$		10	
Room temperature T_a (K)		295.5	Experimental measurement

3.2 Skin injury mathematical modeling

Parametric evaluation of tissue damage was investigated in 1947 by Henriques and Moritz in a series of seminal papers [23], [24]. In their work, the thermal damage was quantified using a dimensionless positive function $\Omega(x,t)$, given by the Arrhenius equation:

$$\Omega(x,t) = A\int_0^t \exp\left(\frac{-E_a}{RT(x,\tau)}\right)d\tau \qquad (5)$$

where A is a pre exponential factor $\left[\text{s}^{-1}\right]$, E_a is the activation energy $\left[\text{J.mole}^{-1}\right]$ and R is the universal gas constant (8.32 $\text{J.mole}^{-1}\text{.K}^{-1}$). One can notice that the pre exponential factor A can be defined as a molecular collision frequency.

While studying *in vivo* pig skin temperature, during a burn with warm water, Henriques and Moritz defined three values of Ω corresponding to three burn degrees [23]:

- $0.53 \le \Omega(x,t) < 1$ describes a first degree of burn,
- $1 \le \Omega(x,t) < 10^4$ is the range for second degree of burn,
- $10^4 \le \Omega(x,t)$ corresponds to a third degree of burn.

In this early works, $A = 3.1\ 10^{98}$ s^{-1} and $E_a = 6.26\ 10^5$ J.mole^{-1}. It is obvious that such empirical parameters have to be implemented with a great circumspection and, more recently, several authors investigating thermal damage of biological tissues have proposed various points of view [25]. Considering the experimental results from Henriques, Fugitt (in 1955) [26] and Wu (in 1982) [27] attempted to improve the method by introducing a two-stage temperature activation model. In 1967 and in 1974, studies of Weaver and Stoll on human skin [28] and of Takata on pig skin permitted to modify A and E_a values [29]. Gaylor and Rocchio in 1989, from a molecular biology point of view, measured the membrane permeability change of mammalian skeletal muscle cell submit to a thermal stress and additional values of A and E_a were suggested [30]. Finally, in 1993 Pearce

et al. studied rat skin and considering histopathology results, a set of coefficients for birefringence loss in skin collagen was proposed [31]. These different values are studied and compared in this paper with the experimental results. Values used are gathered in Table 7.

Table 7 – Thermal damage model: parameters A and E_a

Model	Temperature range [K]	E_a $\left[\text{J.mole}^{-1}\right]$	A $\left[\text{s}^{-1}\right]$
Fugitt [26]	$T \leq 328$	$6.27\ 10^5$	$3.1\ 10^{98}$
	$T > 328$	$2.96\ 10^5$	$5.0\ 10^{45}$
Gaylor [30]	All T	$2.4\ 10^5$	$2.9\ 10^{37}$
Henriques [22], [24]	All T	$6.27\ 10^5$	$3.1\ 10^{98}$
Pearce [31], [32]	All T	$3.06\ 10^5$	$1.606\ 10^{45}$
Takata [29]	$T \leq 323$	$4.18\ 10^5$	$4.322\ 10^{64}$
	$T > 323$	$6.69\ 10^5$	$9.389\ 10^{104}$
Weaver and Stoll [28]	$T \leq 323$	$7.82\ 10^5$	$2.185\ 10^{124}$
	$T > 323$	$3.27\ 10^5$	$1.823\ 10^{51}$
Wu [27]	$T \leq 326$	$6.27\ 10^5$	$3.1\ 10^{98}$
	$T > 326$	$(6.27\text{-}0.0051(T\text{-}53))\ 10^5$	$3.1\ 10^{98}$

Once the thermal damage $\Omega(x,t)$ estimated, it is important to take into account its potential effect on the blood perfusion rate ω_i in $\left[\text{s}^{-1}\right]$. Blood circulatory evolution during temperature increase has been investigated by few authors. Abraham and Sparrow [33] describe a relation between blood circulatory (ω_i) and tissues damage (Ω). However, relation $\omega_i(\Omega)$ is quite difficult to establish. In the following, blood perfusion throughout the heating process for a porcine model [18] has been modeled as follows:

$$\begin{aligned} \omega(\Omega) &= \left(1 + 25\Omega - 260\Omega^2\right)\omega_0 \quad && \Omega \in [0, 0.1] \\ \omega(\Omega) &= (1-\Omega)\,\omega_0 && \Omega \in\ ]0.1, 1] \\ \omega(\Omega) &= 0 && \Omega > 1 \end{aligned}$$

In the first of the previous equations, increase in the perfusion rate is described as tissue is moderately heated, with vasodilatation due to inflammation. In the second equation, while the heating process persists, blood flow decreases as the vasculature begins to shut down (thrombosis/necrosis). The term ω_0 is the rate of perfusion in totally undamaged tissue [33], [34]. According to the referenced work, ω_0 is $8.3\ 10^{-3}\ \text{s}^{-1}$ in the dermis ($5.3\ 10^{-4}\ \text{s}^{-1}$ in the hypodermis).

In the following paragraph, numerical simulation results are presented in order to investigate the reliability of such numerical approach in the specific context of damage estimation caused by laser occurrences.

3.3 Estimation of damage caused by burn: an example…

In order to validate the thermal damage model, skin temperatures were calculated using the finite element method (Comsol solver and matlab software). Predicted damages are quite different according to authors set of parameters (A and E_a) and in several situations are not in accordance with histological results. For example in Table 8, results are presented for effects occurred by the 1940 nm laser ($14\ \text{kW.m}^{-2}$).

Table 8 – Predicted damages 1940 nm laser.

Authors	Calculated temperatures				Measured temperatures				Histological grade (histopathology)			
	1 s	5 s	10 s	20 s	1 s	5 s	10 s	20 s	1 s	5 s	10 s	20 s
Fugitt	0	0	0	2	0	0	2	2				
Gaylor	0	0	2	2	0	0	2	2				
Henriques	0	0	0	2	0	0	2	3				
Pearce	0	0	0	0	0	0	0	2	0	0	2+	3
Takata	0	0	0	2	0	0	2	3				
Weaver and Stoll	0	0	0	2	0	0	2	2				
Wu	0	0	3	3	0	3	3	3				

Considering damage predictions, in the studied configuration, one can notice that:

- with measured temperature:
  - Pearce criterion is not relevant since burn damage is drastically underestimated,
  - Fugitt, Gaylor, Weaver and Stoll criteria lightly underestimate damage,
  - Henriques and Takata criteria seem to be adequate for burn prediction,
  - Wu criterion overestimates the dangerous nature of the laser exposure.
- with calculated temperature (considering the mathematical predictive model):
  - Pearce criterion is not able to predict damage (absence of lesion),
  - Fugitt, Henriques, Takata, Weaver and Stoll criteria drastically underestimate damage,
  - Gaylor criterion lightly underestimates burn damages
  - Wu criterion seems to be more relevant.

It is important to notice that predicted burn degree depends on temperature time history and that if temperature evolution is questionable then predicted damage is meaningless. Generally, for experimental configurations presented in this communication, mathematical model tends to underestimate the damage caused by laser.

4. Concluding remarks

Considering two lasers (808 nm and 1940 nm), *in vivo* experimentations have been performed on pigs in order to investigate several exposure duration and power. Main result of experimental campaign is that considering measured skin temperatures and induced burns (histological analysis), it is established that skin behavior is quite different according to the laser wavelength. It has been shown that a more surface heating is obtained considering a 1940 nm laser. Moreover, histological analysis has established that for a given irradiance and a given laser exposure duration, burns induced by 808 nm are less damageable.

A numerical predictive tool has been investigated in order to evaluate the damage level. Taken into account absorption and scattering of laser beam (in a unique parameter $\beta(\lambda)$ which depends on the laser wavelength), it allows to compare lesion caused by both of the lasers. The use of an injury-dependent perfusion in such simulations is also taken into account.

Several outlooks have to be considered in order to improve the numerical approach reliability.

Firstly, even if the model structure seems to be relevant in order to describe this type of irradiation, improvements have to be proposed. In such a way, a methodology based on numerical design of experiment [35] can be implemented in order to investigate the effect of each mathematical model parameter uncertainty. In fact, numerous parameters as the blood perfusion rate in undamaged tissue, the thermal diffusivity of the three skin layers or coefficients for the damage evaluation are issued from literature and present questionable variability.

Secondly, investigations have to be performed about model parameters usually considered as constant all along the burn phenomenon. This strong assumption sounds dubious. In the proposed model, only blood circulatory is assumed to depend on injury level. Nevertheless, for second or third degree burns, one can consider more physiological modifications and this specific point has to be taken into account for model properties (optical, mechanical, thermal). For example, Laufer et al. [36] show that optical properties of human dermis and hypodermis are temperature dependent over a wavelength range of 650-1000 nm. In particular, significant changes are observed for scattering coefficient. Moreover, effect of optical properties of hair follicles and their impact on the skin heating could be investigated.

Finally, in order to validate the proposed mathematical model for further laser wavelengths, an experimental test bench using a 10.6 μm laser is actually tested in our laboratory.

5. References

[1] Jackson SD, Lauto A. Diode-pumped fiber lasers: a new clinical tool?, Lasers Surg. Med., vol. 30, no. 3, 2002, pp. 184-190.

[2] Jacques SL. Role of tissue optics and pulse duration on tissue effects during high-power laser irradiation, Appl. Opt., vol. 32, no. 13, 1993, pp. 2447-2454.

[3] Chen B, O'Dell DC, Thomsen SL, Rockwell BA,Welch AJ., Porcine skin ED50 damage thresholds for 2,000 nm laser irradiation, Lasers Surg. Med., vol. 37, no. 5, 2005, pp. 373-381.

[4] Maher EF. Transmission and absorption coefficients for ocular media of the Rhesus monkey, in Report SAM-TR-78-32, San Antonio, TX: Brooks Air Force Base, 1978.

[5] Winburn DC. Practical laser safety, ed. Marcel Dekker Inc., 2nd revised edition, in Occupational Safety and Health collection, 1989, pp. 256.

[6] Jaunich M, Raje S, Kim K, Mitra K, Guo Z. Bio-heat transfer analysis during short pulse laser irradiation of tissues, International Journal of Heat and Mass Transfer, vol. 51, n° 23-24, pp. 5511-5521, 2008.

[7] Forges PD. Vascular supply of the skin and hair in swine, in Hair Growth - Advances in Biology of Skin, Oxford: Pergamon, 1967, pp. 419-432.

[8] Sullivan TP, Eaglstein WH, Davis SC, Mertz P. The pig as a model for human wound healing, Wound Rep. Reg., vol. 9, no.2, 2001, pp. 66-76.

[9] Chen B, Thomsen SL, Thomas RJ, Oliver J, Welch AJ. Histological and modeling study of skin thermal injury to 2.0 µm laser irradiation, Lasers Surg. Med., vol. 40, no. 5, 2008, pp. 358-370.

[10] Johnson NN, Abraham JP, Helgeson ZI, Minkowycz WJ, Sparrow EM. An Archive of Skin-Layer Thicknesses and Properties and Calculations of Scald Burns with Comparisons to Experimental Observations, J. of Thermal Science and Engineering Applications, Vol. 3, paper no. 011003, 2011.

[11] Abraham JP, Minkowycz WJ, Hennessey MP. A simple Algebraic Model to Predict Burn Depth and Injury, Int. Comm. Heat Mass Transfer, (in press).

[12] Breaban F, Coutouly JF, Deprez P, Deffontaine A. Study and construction of an homogeniser for high power laser beam, Lasers Eng., vol. 11, no. 2, 2001, pp. 77-89.

[13] Pennes HH. Analysis of tissue and arterial blood temperatures in the resting normal human forearm, J. Appl. Physiol., vol. 85, no. 1, 1948, pp. 5-34.

[14] Torres JH, Motamedi M, Pearce JA, Welch AJ. Experimental evaluation of mathematical models for predicting the thermal response of tissue to laser irradiation, Appl. Opt. vol. 32, n° 4, pp. 597-606, 1993.

[15] Incropera FP, Dewitt DP. Fundamentals of Heat and mass transfer, 5th ed., John Wiley & Sons, New York, 2001.

[16] Diaz SH, Aguilar G, Lavernia EJ, Wong BJF. Modeling the thermal response of porcine cartilage to laser irradiation, IEEE J. Quantum Electron. vol. 7, n° 6, pp. 944-951, 2001.

[17] Stolwijk JAJ, Hardy JD. Skin and subcutaneous temperature changes during exposure to intense thermal radiation, J. Appl. Physiol. vol. 20, pp. 1006-1013, 1965.

[18] Knudsen M, Overgaard J. Identification of thermal model for human tissue, IEEE Trans. Biomed. Eng. vol. 33, n° 5, pp. 477-485, 1986.

[19] Cohen ML. Measurement of the thermal properties of human skin. A review, J. Invest. Dermatol. vol. 69, n° 3, pp. 333-338, 1977.

[20] Diller KR, Hayes LJ. A finite element model of burn injury in blood-perfused skin, J. Biomech. Eng. vol. 105, pp. 300-307, 1983.

[21] Sipe JE. Development of an instrumented dynamic mannequin test to rate the thermal protection provided by protective clothing, Ph.D. thesis Worcester Polytechnic Institute, 1994.

[22] Lormel C. Analyse d'un système mathématique modélisant les interactions laser-peau pour la prédiction de la brûlure, Ph.D. thesis Perpignan, France, 2005.

[23] Moritz AR, Henriques FC. Studies of thermal injury II. The relative importance of time and surface temperature in the causation of cutaneous burns, Am. J. Pathol. vol. 23, pp. 695-720, 1947.

[24] Henriques FF. Studies of thermal injury V: The predictability and the significance of thermally induced rate processes leading to irreversible epidermal injury, Arch. Pathol. vol. 43, pp. 489-502, 1947.

[25] Wright NT. On a relationship between the Arrhenius parameters from thermal damage studies, Journal of biomechanical engineering- Transactions of the ASME, vol. 125, n°2, pp. 300-304, 2003.

[26] Fugitt CE. A rate process of thermal injury, Armed Forces Special Weapons Project AFSWP-606, 1955.

[27] Wu YC. A modified criterion for predicting thermal injury, National Bureau of Standards, Washington, District of Columbia, 1982.

[28] Weaver JA, Stoll AM. NADC Memo Report 6708, United Stated Naval Air Development Center, Johnsville, Pennsylvania, 1967.

[29] Takata AN. Development of criterion for skin burns, Aerospace Med. vol. 45, pp. 634-637, 1974.

[30] Gaylor DC. Physical mechanisms of cellular injury in electrical trauma, Ph.D. thesis Massachusetts Institute of Technology, 1989.
[31] Pearce JA, Thomsen SL. Vijverberg H, McMurray TJ. Kinetics for birefringence changes in thermally coagulated rat skin collagen, in Proc SPIE 1876, 180-185, 1993.
[32] Pearce JA, Thomsen SL. Thermal damage parameters from laser coagulation experiments, Progress in Biomedical Optics and Imaging (SPIE), San José, California, USA, 4954, pp. 58-63, 2003.
[33] Abraham JP, Sparrow EM. A thermal-ablation bioheat model including liquid-to-vapor phase change, pressure-and necrosis-dependent perfusion, and moisture-dependent properties, Int. J. Heat Mass Trans. vol. 50, pp. 2537-2544, 2007.
[34] Baldwin SA, Pelman A, Bert JL. A heat transfer model of thermal balloon endometrial ablation, Ann. Biomed. Eng. vol. 29, pp. 1009-1018, 2001.
[35] Autrique L, Lormel C. Numerical design of experiment for sensitivity analysis - Application to skin burn injury prediction, IEEE Trans. Biomed. Eng. vol. 55, n° 4, pp. 1279-1290, 2008.
[36] Laufer J, Simpson R, Kohl M, Essenpreis M, Cope M. Effect of temperature on the optical properties of ex vivo human dermis and subdermis, Phys. Med. Biol. vol. 43, pp. 2479-2489, 1998.